Strange-quark contribution to the ratio of neutral- to charged-current cross sections in neutrino-nucleus scattering

B. I. S. van der Ventel[1,*] and J. Piekarewicz[2,†]

[1]*Department of Physics, Stellenbosch University, Stellenbosch 7600, South Africa*
[2]*Department of Physics, Florida State University, Tallahassee FL 32306, USA*

(Dated: February 9, 2008)

arXiv:nucl-th/0506071v1 23 Jun 2005

Abstract

A formalism based on a relativistic plane wave impulse approximation is developed to investigate the strange-quark content (g_A^s) of the axial-vector form factor of the nucleon via neutrino-nucleus scattering. Nuclear structure effects are incorporated via an accurately calibrated relativistic mean-field model. The ratio of neutral- to charged-current cross sections is used to examine the sensitivity of this observable to g_A^s. For values of the incident neutrino energy in the range proposed by the FINeSSE collaboration and by adopting a value of $g_A^s = -0.19$, a 30% enhancement in the ratio is observed relative to the $g_A^s = 0$ result.

PACS numbers: 24.10.Jv,24.70.+s,25.30.-c

*Electronic address: bventel@sun.ac.za
†Electronic address: jorgep@csit.fsu.edu

I. INTRODUCTION

In a desperate effort to salvage the conservation of energy and angular momentum, Wolfgang Pauli postulated the existence of the neutrino: a neutral and (almost) massless particle that he feared will never be detected. Seventy five years later and with three neutrino families firmly established, neutrino physics in the 21st century has taken center stage in fields as diverse as cosmology, astro, nuclear, and particle physics. With the commission of new neutrino observatories and facilities for the study of solar, atmospheric, and reactor neutrinos, conclusive evidence now exists in favor of neutrino oscillations. Although neutrino-oscillation experiments have now evolved from the discovery into the precision phase, important questions remain unanswered [1]. Depending on these answers, a radical modification to the standard model of particle physics may be required. At the very least, neutrino oscillations already demand a mild extension to the standard model: in the standard model the *individual* lepton numbers must be conserved.

The discovery of neutrino oscillations established two incontrovertible facts: a) that neutrinos have mass and that these masses can not all be equal and b) that the three known neutrinos ν_e, ν_μ, and ν_τ are linear combinations of three neutrino mass eigenstates (commonly referred as ν_1, ν_2, and ν_3). Note that due to the very small neutrino masses, oscillation experiments are sensitive to only the *squared mass difference* (Δm^2) of the mass eigenstates. Further, the unitary matrix linking the flavor to the mass eigenstates has a well-known counterpart in the quark sector: the CKM matrix. While precision experiments have started to determine squared mass differences and mixing angles, a strong, vibrant, and interdisciplinary program is now being established to tackle the myriad of remaining open questions [1]. Among these are: What is the mass hierarchy? Is the neutrino a Dirac or Majorana particle? Does the neutrino matrix contain a CP-violating phase that may explain our matter-dominated Universe? Is there a need for additional "sterile" neutrinos?

The apparent need for an additional sterile neutrino stems from two older experiments. The first one in 1989 measured the total and partial (into hadrons and charged leptons) widths of the Z^0 boson at the large electron-positron (LEP) collider at CERN and extracted the number of neutrinos flavors to be $N_\nu = 3.00 \pm 0.08$; note that a more recent analysis reports $N_\nu = 2.984 \pm 0.008$ [2]. The second experiment was a 1995 neutrino-oscillation experiment at the Liquid Scintillator Neutrino Detector (LSND) at the Los Alamos National Laboratory [3]. This experiment reported evidence of $\bar{\nu}_\mu \rightarrow \bar{\nu}_e$ oscillation, but with a squared mass difference that is too large — and thus inconsistent — with the two *independent* values extracted from solar, atmospheric, and reactor experiments. Simply put, for three neutrino flavors the algebraic relation $\Delta m^2_{21} + \Delta m^2_{32} = \Delta m^2_{31}$ must be satisfied, yet $\Delta m^2_{\rm sol} + \Delta m^2_{\rm atm} \neq \Delta m^2_{\rm LSND}$. The most favorable scenario that accommodates three independent Δm^2 values is the addition of a sterile neutrino. Yet other possibilities exist: the LSND analysis may be incorrect. It is the primary goal of the Booster Neutrino Experiment (BooNE and its first phase MiniBooNE) at Fermilab to confirm the LSND result.

While MiniBooNE's primary goal is to confirm the LSND result, this unique facility is also ideal for the study of supernova neutrinos, neutrino-nucleus scattering, and hadronic structure. An ambitious experimental program — the Fine-grained Intense Neutrino Scattering Scintillator Experiment (FINeSSE) — aims to measure the strange-quark contribution to the spin of the nucleon [4, 5, 6]. FINeSSE is part of a larger program started in the late 80's that attempts to answer a fundamental nucleon-structure question: how do the non-valence ("sea") quarks — particularly the strange quarks — contribute to the observed properties

of the nucleon? To date, the role of strange quarks in the nucleon remains a contentious issue and one that remains a subject of intense activity all over the world. In an attempt to find a satisfactory answer to this fundamental question, a number of reactions have been proposed. These include: (i) deep inelastic scattering of neutrinos on protons [7, 8], (ii) deep inelastic scattering of polarized charged leptons [9], (iii) pseudoscalar meson scattering on a proton [10], and (iv) parity-violating electron scattering [11, 12]. Part of the controversy arises because these reactions do not all reach similar conclusions. For example, both reactions (i) and (ii) suggest a non-zero strangeness contribution, in contrast to reaction (iv) that indicates a strange quark contribution to the charge and magnetic moment consistent with zero. Parity-violating electron scattering in particular has received extensive experimental attention as in the SAMPLE Collaboration at the MIT-Bates accelerator [13], the HAPPEX Collaboration at the Jefferson Laboratory [14], and the A4 Collaboration at the MAMI facility in Mainz [15]. However, theoretical investigations have shown that large radiative corrections and nuclear-structure effects impact negatively on the extraction of strange-quark matrix elements [16, 17, 18].

Neutrino-induced reactions provide a viable alternative to parity-violating electron scattering. While the latter is primarily sensitive to the strange electric and magnetic form factors of the nucleon, the former is particularly sensitive to the axial-vector form factor of the proton — through the combination $(\Delta u - \Delta d - \Delta s + \Delta c - \Delta b + \Delta t)$. This sensitivity is the result of the small weak-vector charge of the proton $(1 - 4\sin^2\theta_{\rm W} \simeq 0.08)$ and the suppression of the weak anomalous magnetic moment at small Q^2. In the above expression the heavy quark flavors (c, b, and t) can be eliminated using a well-defined renormalization group procedure [19, 20]. Further, the isovector combination $(\bar{u}\gamma_\mu\gamma_5 u – \bar{d}\gamma_\mu\gamma_5 d)$ is constrained from neutron beta decay. This leaves the (assumed isoscalar) strange-quark contribution to the spin of the proton Δs to be determined from the elastic neutrino-proton reaction. Yet an absolute cross-section measurement of this reaction is an experimental challenge due to difficulties in the determination of the absolute neutrino flux. An attractive alternative has been proposed by Garvey and collaborators [21, 22] in which the extraction of Δs proceeds through a measurement of the *ratio* of proton-to-neutron cross sections in neutral-current (NC) neutrino-nucleon scattering. This ratio is defined by the following expression:

$$R(p/n) = \frac{\sigma(\nu p \to \nu p)}{\sigma(\nu n \to \nu n)} \; . \tag{1}$$

This ratio is very sensitive to the strange-quark contribution to the spin of the nucleon as Δs [or $g_A^s \equiv G_A^{(s)}(Q^2 = 0)$] interferes with the isovector contribution ($G_A^{(3)}$) with one sign in the numerator and with the opposite sign in the denominator [see Eq. 31]. Unfortunately, $R(p/n)$ is difficult to measure with the desired accuracy due to experimental difficulties associated with neutron detection [6]. It is for this reason that FINeSSE will focus initially on the neutral- to charged-current ratio (NC/CC):

$$R(NC/CC) = \frac{\sigma(\nu p \to \nu p)}{\sigma(\nu n \to \mu^- p)} \; . \tag{2}$$

This ratio is "simply" determined from counting the number of events with an outgoing proton and missing mass relative to those events with an outgoing proton and a muon. Note that the CC reaction, being purely isovector, is insensitive to Δs. As such, $R(NC/CC)$ is about a factor of two less sensitive to Δs than $R(p/n)$.

From a theoretical perspective extracting Δs from the ratio of cross sections is also attractive. As a large number of the scattering events at FINeSSE will be from nucleons bound to a Carbon nucleus, it is important to understand nuclear-structure corrections. This issue came to light in experiment E374 at the Brookhaven National Laboratory (BNL) where it was found that 80% of the events involved neutrino scattering off carbon atoms, while only 20% were from free protons. As nuclear-structure corrections in $R(NC/CC)$ appear to be insensitive to final-state interactions between the outgoing proton and the residual nucleus [23, 24], the ratio $R(NC/CC)$ may be accurately computed using a much simpler plane-wave formalism. Indeed, in Sec. II we will show how the cross section ratio $R(NC/CC)$ in Carbon computed in a plane-wave formalism may be expressed in a form that closely resembles the "Feynman-trace" approach used to calculate the cross section from free nucleons. We note in closing that the new generation of neutrino experiments will require a thorough understanding of neutrino-nucleus interactions since the detectors often contain complex nuclei. Experimental and theoretical work related to neutrino scattering from light and heavier nuclear targets may be found in Refs. [25, 26, 27, 28, 29, 30, 31, 32].

Our paper has been organized as follows. In Sec. II we briefly review the formalism developed in Ref. [33] for the neutral-current case and point out the main modifications required to make it applicable to charged-current neutrino-nucleus scattering. Our main results — with a focus on the sensitivity of $R(NC/CC)$ to Δs — are presented in Sec. III. Finally, we summarize the main points of this work in Sec. IV.

II. FORMALISM

In this section the formalism for the description of charged-current neutrino-nucleus scattering is presented. As the basic outline follows closely the neutral-current formalism developed in Ref. [33], we present a brief review that focusses on those modifications that arise from a finite muon mass.

A. Cross section in terms of the leptonic and hadronic tensors

The lowest-order Feynman diagram for the knockout of a bound proton via the charged-current reaction $[\nu + X(Z,A) \rightarrow \mu^- + p + X(Z-1, A-1)]$ is shown in Fig. 1. Here the initial four-momentum of the (left-handed) neutrino is k while the four-momentum and helicity of the outgoing muon are k' and h', respectively. The reaction proceeds via the exchange of a virtual W^+ boson with four-momentum $q = (\omega, \mathbf{q})$. The kinematical variables defining the hadronic arm are the four-momentum of the target (P) and residual nucleus (P'). Finally, p' and s' denote the four-momentum and spin component of the ejectile proton. Energy-momentum conservation demands that:

$$q = k - k' = p' + P' - P \; . \tag{3}$$

The dynamical information for this reaction is contained in the transition matrix element given by

$$\begin{aligned} -i\mathcal{M} \; = \; & \left\{ \overline{\mu}(\mathbf{k}', h') \left[\frac{-ig}{2\sqrt{2}} \left(\gamma^\mu - \gamma^\mu \gamma^5 \right) \right] \nu(\mathbf{k}) \right\} i\mathcal{D}_{\mu\nu}(q) \\ & \left\{ \langle \, p', s' ; \; \Psi_f(P') \left| \frac{-ig}{2\sqrt{2}} \cos\theta_C \, \hat{J}^\nu(q) \right| \Psi_i(P) \, \rangle \right\} . \end{aligned} \tag{4}$$

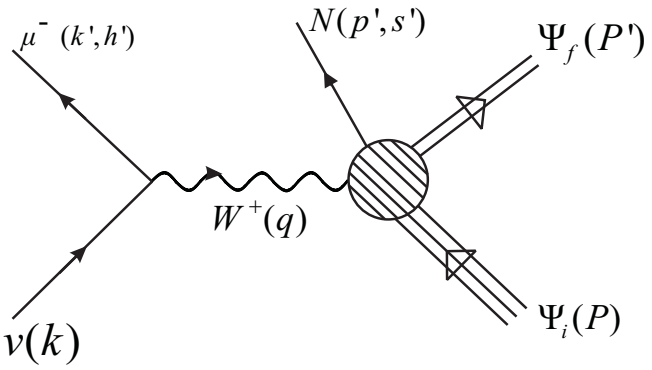

FIG. 1: Lowest-order Feynman diagram for charged-current neutrino-nucleus scattering.

In Eq. (4) the initial and final nuclear states are denoted by $\Psi_i(P)$ and $\Psi_f(P')$, respectively. Furthermore, g is the weak coupling constant, θ_C is the Cabbibo angle ($\cos\theta_C = 0.974$), and $\hat{J}^\nu(q)$ is the weak nuclear current operator. As only low-momentum transfers ($-q_\mu q^\mu \equiv Q^2 \ll M_W^2$) will be considered, the following approximation is valid

$$\mathcal{D}_{\mu\nu}(q) = \frac{-g_{\mu\nu} + q_\mu q_\nu / M_W^2}{q^2 - M_W^2} \longrightarrow \frac{g_{\mu\nu}}{M_W^2} \, . \tag{5}$$

Using this expression the transition matrix element may be written as

$$\mathcal{M} = \frac{G_F}{\sqrt{2}} \cos\theta_C \left[\overline{\mu}(\mathbf{k}', h')\gamma_\mu(1-\gamma^5)\nu(\mathbf{k})\right] \left[\langle p', s'; \Psi_f(P') \Big| \hat{J}^\mu(q) \Big| \Psi_i(P)\rangle\right] \, , \tag{6}$$

where the Fermi coupling constant G_F has been introduced via

$$\frac{G_F}{\sqrt{2}} = \frac{g^2}{8M_W^2} \, . \tag{7}$$

In Eq. (6) $\mu(\mathbf{k}', h')$ is the Dirac spinor for the outgoing muon expressed in the helicity representation. That is, (suppressing "prime" indices for clarity),

$$\mu(\mathbf{k}, h) = \sqrt{\frac{E_k + m}{2E_k}} \begin{pmatrix} \phi_h(\widehat{\mathbf{k}}) \\ h\dfrac{k}{E_k + m}\phi_h(\widehat{\mathbf{k}}) \end{pmatrix} \, , \quad \left(E_k = \sqrt{k^2 + m^2} \, ; \, k = |\mathbf{k}|\right) \, , \tag{8}$$

where $\phi_{h=\pm1}(\widehat{\mathbf{k}})$ are two-component Pauli spinors given by

$$\phi_{h=+1}(\widehat{\mathbf{k}}) = \begin{pmatrix} \cos(\theta/2) \\ \sin(\theta/2)\, e^{i\phi} \end{pmatrix} \, , \quad \phi_{h=-1}(\widehat{\mathbf{k}}) = \begin{pmatrix} -\sin(\theta/2)\, e^{-i\phi} \\ \cos(\theta/2) \end{pmatrix} \, . \tag{9}$$

Here m denotes the muon mass, and θ and ϕ are the polar and azimuthal angles of the muon momentum. The neutrino spinor $\nu(\mathbf{k})$ is directly obtained from the above expressions by setting the fermion mass to $m = 0$ and the helicity to $h = -1$. Note that left/right projection operators on plus/minus helicity states do not vanish in general due to the finite muon mass. That is,

$$\mathcal{P}_{L/R}\, \mu(\mathbf{k}, h = \pm 1) \equiv \frac{1}{2}(1 \mp \gamma^5)\mu(\mathbf{k}, h = \pm 1) = \mathcal{O}(m/k) \neq 0 \, . \tag{10}$$

Further, we have adopted a non-covariant normalization for the Dirac spinors of Eq. (8),

$$\mu^\dagger(\mathbf{k},h)\mu(\mathbf{k},h') = \bar{\mu}(\mathbf{k},h)\gamma^0\mu(\mathbf{k},h') = \delta_{hh'} \ , \tag{11}$$

a choice that is in accordance with the standard normalization of the bound-state spinor [34] and that is given by

$$\int \mathcal{U}_\alpha^\dagger(\mathbf{r})\,\mathcal{U}_\alpha(\mathbf{r})\,d^3\mathbf{r} = 1 \ . \tag{12}$$

Following Ref. [33] the differential cross section can now be written as

$$d\sigma = \frac{G_F^2\cos^2\theta_C}{2(2\pi)^5} d^3\mathbf{k}' d^3\mathbf{p}' \delta(E_k + M_A - E_{k'} - E_{p'} - E_{P'})\ell_{\mu\nu}W^{\mu\nu} \ , \tag{13}$$

where the leptonic tensor is given by

$$\ell_{\mu\nu} = \mathrm{Tr}\left[(\gamma_\mu - \gamma_\mu\gamma_5)\left(\nu(\mathbf{k})\overline{\nu}(\mathbf{k})\right)(\gamma_\nu - \gamma_\nu\gamma_5)\left(\mu(\mathbf{k}',h')\overline{\mu}(\mathbf{k}',h')\right)\right] \ , \tag{14}$$

and a discussion of the hadronic tensor $W^{\mu\nu}$ is postponed until the next section.

We conclude this section with the evaluation of the leptonic tensor. To do so, both matrices $\nu\overline{\nu}$ and $\mu\overline{\mu}$ in Eq. (14) are first expressed in terms of Dirac matrices. For the case of the massive muon we obtain

$$\mu(\mathbf{k}',h')\overline{\mu}(\mathbf{k}',h') = \frac{(\not{k}' + m)}{2E_{k'}}\left[\frac{1}{2}(1 + h'\gamma^5\not{s})\right] \ , \tag{15}$$

where the four-component spin vector is given by

$$s^\mu \equiv s^\mu(\mathbf{k}') = \frac{1}{m}\left(k', E_{k'}\,\widehat{\mathbf{k}'}\right) \ . \tag{16}$$

The corresponding expression for the massless left-handed neutrino may be obtained from the above equations by setting the helicity to $h = -1$ and by taking the massless ($m \to 0$) limit. Note that in the massless limit $ms^\mu \to k'^\mu$. Thus we obtain,

$$\nu(\mathbf{k})\overline{\nu}(\mathbf{k}) = \frac{\not{k}}{2E_k}\left[\frac{1}{2}(1+\gamma^5)\right] \tag{17}$$

Finally, by substituting the above expressions into the leptonic tensor of Eq. (14), which in turn we separate into ($\mu \leftrightarrow \nu$) symmetric and antisymmetric parts,

$$\ell^{\,\mu\nu} \equiv \ell_S^{\,\mu\nu} + \ell_A^{\,\mu\nu} \ , \tag{18}$$

we obtain

$$\ell_S^{\,\mu\nu} = \frac{2}{kE_{k'}}\left(k^\mu K'^\nu + K'^\mu k^\nu - g^{\mu\nu}k\cdot K'\right) \ , \tag{19a}$$

$$\ell_A^{\,\mu\nu} = -\frac{2i}{kE_{k'}}\varepsilon^{\mu\nu\alpha\beta}k_\alpha K'_\beta \ . \tag{19b}$$

Note that in the above expressions the following four-vector has been introduced:

$$K' \equiv \frac{1}{2}(k' - h'ms) \underset{m=0}{\longrightarrow} k'\delta_{h',-1} \ , \tag{20}$$

where the last expression denotes the massless limit. Hence, in the $m \to 0$ limit the leptonic tensor vanishes for positive-helicity ($h'=+1$) but for negative-helicity ($h'=-1$) goes over to Eq. (17) of Ref. [33]. Finally, note that the following convention was adopted [35]:

$$\mathrm{Tr}\left(\gamma^5\gamma^\mu\gamma^\nu\gamma^\alpha\gamma^\beta\right) = 4i\,\varepsilon^{\mu\nu\alpha\beta}\ , \quad (\varepsilon^{0123}=-1,\ \varepsilon_{0123}=+1)\ . \tag{21}$$

We close this section with a comment on the conservation (or rather lack-thereof) of the leptonic tensor. While the antisymmetric component satisfies

$$q_\mu \ell_A^{\mu\nu} = \ell_A^{\mu\nu} q_\nu = 0\ , \tag{22}$$

due to the antisymmetric property of the Levi-Civita tensor, this is no longer true for the symmetric part due to the finite muon mass. That is,

$$q_\mu \ell_S^{\mu\nu} \neq 0 \quad \text{and} \quad \ell_S^{\mu\nu} q_\nu \neq 0\ . \tag{23}$$

B. Differential cross section in terms of nuclear structure functions

In Eq. (13) of the previous section it was shown that the differential cross section for the CC reaction may be written as a contraction of the leptonic tensor with the hadronic tensor, where the latter is defined in terms of the expectation value of the weak nuclear operator [see Eq. (6)]. That is,

$$W^{\mu\nu} = \Big[\langle p', s'\,;\Psi_f(P')\Big|\hat{J}^\mu(q)\Big|\Psi_i(P)\rangle\Big]\,\Big[\langle p', s'\,;\Psi_f(P')\Big|\hat{J}^\nu(q)\Big|\Psi_i(P)\rangle\Big]^* \equiv W_S^{\mu\nu} + W_A^{\mu\nu}\ . \tag{24}$$

Although the general form of the hadronic tensor was introduced and discussed in detail in Ref. [33], some of its most salient features are underscored here for completeness. For the case of unpolarized proton emission, the hadronic tensor may be written in terms of thirteen independent structure functions,

$$\begin{aligned} W_S^{\mu\nu} &= W_1 g^{\mu\nu} + W_2 q^\mu q^\nu + W_3 P^\mu P^\nu + W_4\, p'^\mu p'^\nu \\ &+ W_5(q^\mu P^\nu + P^\mu q^\nu) + W_6(q^\mu p'^\nu + p'^\mu q^\nu) + W_7(P^\mu p'^\nu + p'^\mu P^\nu)\ , \qquad \text{(25a)} \\ W_A^{\mu\nu} &= W_8(q^\mu P^\nu - P^\mu q^\nu) + W_9(q^\mu p'^\nu - p'^\mu q^\nu) + W_{10}(P^\mu p'^\nu - p'^\mu P^\nu) \\ &+ W_{11}\varepsilon^{\mu\nu\alpha\beta} q_\alpha P_\beta + W_{12}\varepsilon^{\mu\nu\alpha\beta} q_\alpha p'_\beta + W_{13}\varepsilon^{\mu\nu\alpha\beta} P_\alpha p'_\beta\ . \qquad \text{(25b)} \end{aligned}$$

Note that all structure functions are functions of the four Lorentz-invariant quantities, $q^\mu q_\mu \equiv -Q^2$, $q\cdot P$, $q\cdot p'$, and $P\cdot p'$. Details on the contraction between the leptonic and hadronic tensors

$$\ell_{\mu\nu}\, W^{\mu\nu} \ = \ \ell^S_{\mu\nu} W_S^{\mu\nu} + \ell^A_{\mu\nu} W_A^{\mu\nu}\ , \tag{26}$$

have been reserved to Appendix A. Yet we note that the charged-current reaction is now sensitive to the three structure functions W_2, W_5 and W_6. This is in contrast to the neutral-current reaction (see Eq. (22a) of Ref. [33]); the origin of this difference is the non-conservation of the symmetric part of the leptonic tensor due to the finite muon mass [see Eq. (23)]. However, as the antisymmetric part of the leptonic tensor is manifestly conserved, both NC and CC processes are insensitive to the W_8 and W_9 structure functions.

This concludes the model-independent description of charged-current neutrino-nucleus scattering. In summary, the cross section may be parametrized in terms of eleven nuclear-structure functions. In principle, they could be determined by a "super" Rosenbluth separation. In practice, however, this is not possible so we resort to a relativistic mean-field model to obtain explicit expressions for these quantities. This will be done in the next section.

C. Model-dependent evaluation of the cross section

In the previous section a model-independent formalism was presented for charged-current neutrino-nucleus scattering. Specifically, the cross section was written in terms of a set of nuclear structure functions that parametrize our "ignorance" about the strong-interactions physics at the hadronic vertex. However, to proceed any further a number of approximations need to be made in order to obtain a numerically tractable problem.

The first "no-recoil" approximation, detailed in Eqs. (23)–(26) of Ref. [33], is purely kinematical and yields the following expression for the angle-integrated differential cross section:

$$\frac{d\sigma(h')}{dE_{p'}} = \frac{G_F^2 \cos^2\theta_C}{2(2\pi)^4}\, k' E_{k'} p' E_{p'} \int_0^{\pi} \sin\alpha\, d\alpha \int_0^{\pi} \sin\theta\, d\theta \int_0^{2\pi} d\phi \left(\ell_{\mu\nu} W^{\mu\nu}\right) . \tag{27}$$

Here α is the polar angle defining the direction of the outgoing proton having momentum $p' \equiv |\mathbf{p}'|$ and energy $E_{p'} = \sqrt{p'^2 + M^2}$. Similarly, θ and ϕ define the polar and azimuthal angles of the outgoing muon with momentum $k' \equiv |\mathbf{k}'|$ and energy $E_{k'} = \sqrt{k'^2 + m^2}$. (For further details we refer the reader to Fig. 2 of Ref. [33]). Finally, to compare the present charged-current calculation to the neutral-current one, we have integrated over the kinematic variables of the outgoing lepton.

The second approximation concerns the evaluation of the nuclear matrix element

$$J^{\mu} = \langle p', s'; \Psi_f(P') \Big| \hat{J}^{\mu}(q) \Big| \Psi_i(P) \rangle . \tag{28}$$

First, two- and many-body components of the current operator are neglected by assuming that the W-boson only couples to a single bound neutron. Second, two- and many-body rescattering processes are neglected by assuming that the detected proton is associated with the specific bound neutron to which the W-boson had coupled to. Further, as we are confident that distortion effects largely factor out from the ratio of cross sections [23, 24], final-state interactions between the outgoing proton and the residual nucleus will be neglected. Finally, the impulse approximation is invoked by assuming that the weak charged-current operator for a nucleon in the nuclear medium retains its free-space form. That is,

$$\hat{J}_{\mu} \equiv \hat{J}_{\mu}^{\rm CC} - \hat{J}_{\mu 5}^{\rm CC} = F_1(Q^2)\gamma_{\mu} + iF_2(Q^2)\sigma_{\mu\nu}\frac{q^{\nu}}{2M} - G_A(Q^2)\gamma_{\mu}\gamma_5 . \tag{29}$$

Here M is the nucleon mass and F_1, F_2, and G_A are Dirac, Pauli, and axial-vector nucleon form factors. Note that the pseudoscalar form factor has been neglected, since its contribution is suppressed by the small lepton mass [36]. A detailed discussion of the weak charge current [Eq. (29)] has been reserved to Appendix B. As we have assumed that the ratio of cross sections given in Eqs. (1) and (2) are insensitive to final state interactions between the outgoing proton and the residual nucleus, both initial (bound) and final (free) nucleon propagators may be written in terms of Dirac gamma matrices — rendering the hadronic tensor analytical. Explicit expressions for both propagators and for the analytic (albeit model-dependent) hadron tensor are given in Eqs. (34–38) of Ref. [33].

III. RESULTS

In this section results are presented based on the formalism outlined in Sec. II for charged-changing neutrino scattering from ^{12}C. The angle-integrated differential cross sec-

tion [Eq. (27)] is shown in Fig. 2 as a function of the kinetic energy $T_{p'}$ of the outgoing proton in the laboratory frame for three incident neutrino energies, namely, $E_k = k = 200, 500$ and 1000 MeV. We display separately the contribution to the cross section from the $1p^{3/2}$ (solid and long-dashed–short-dashed lines) and $1s^{1/2}$ (dashed and dotted lines) orbitals computed in a relativistic mean-field approximation using the NL3 parameter set [37]. Note that because of the finite muon mass, both negative ($h' = -1$) and positive ($h' = +1$) helicity muons contribute to the cross section; the two smallest contributions correspond to the positive-helicity case. As the energy of the incident neutrino increases, and consequently also that of the outgoing muon, the positive-helicity contribution (which scales as $m/E_{k'}$) becomes less and less important until it ultimately disappears at large-enough energy. This can already be observed at $E_k = 500$ and 1000 MeV.

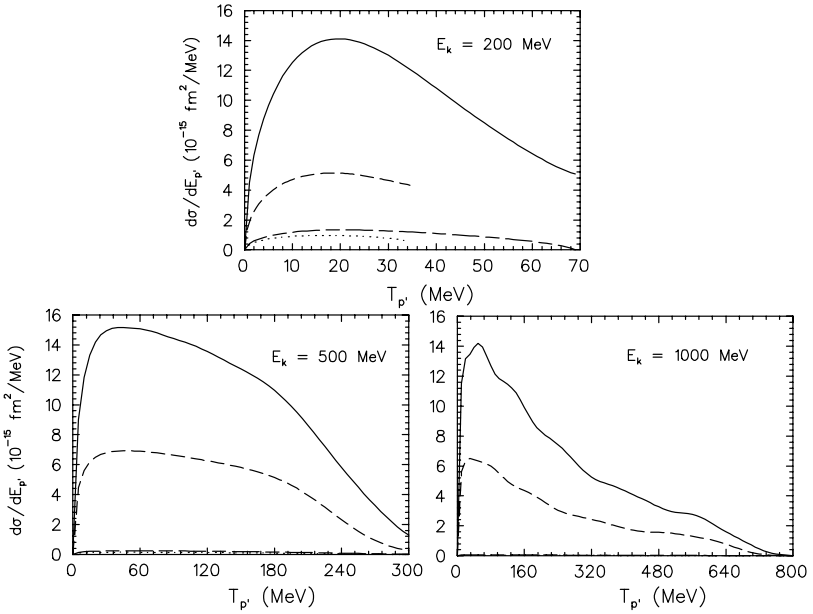

FIG. 2: Differential cross section $d\sigma/dE_{p'}$ [Eq. (27)] as a function of the outgoing proton laboratory kinetic energy $T_{p'}$. The solid and dashed lines denote the contributions from the $1p^{3/2}$ and $1s^{1/2}$ neutron orbitals in ^{12}C to the negative-helicity ($h = -1$) cross section. The long-dashed–short-dashed and dotted lines are the corresponding contributions for positive helicity ($h = +1$). The three considered incident neutrino energies are $E_k = 200, 500$, and 1000 MeV.

For the elementary process $\nu + n \longrightarrow \mu^- + p$, the threshold laboratory energy of the incident neutrino is approximately 112 MeV. An additional kinematical constraint that is strongly affected by binding energy corrections follows from energy conservation. Using the fact that $E_{k'} \geq m$ we obtain

$$E_k + (M + E_B) \geq m + (T_{p'} + M) \implies T_{p'} \leq E_k - E_B - m \,, \tag{30}$$

where E_B is the (positive) binding energy of the neutron. For ^{12}C, the NL3 parameter set predicts $E_B(1s^{1/2}) \approx 53$ MeV and $E_B(1p^{3/2}) \approx 19$ MeV. For the particular case of a neutrino incident energy of $E_k = 200$ MeV, the cross section displays a sharp cut-off for the knockout of the $1s^{1/2}$ neutron at an energy of $T_{p'} \approx 40$ MeV. For higher incident neutrino energies, the maximum allowed value for the kinetic energy of the outgoing proton is already sufficiently large to allow the cross section to fall off smoothly to (almost) zero. Our subsequent results

will only focus on incident neutrino energies of 500 and 1000 MeV, as the ratio $R_{NC/CC}$ defined in Eq. (2) will be measured by the FINeSSE collaboration with neutrinos in that energy range [6].

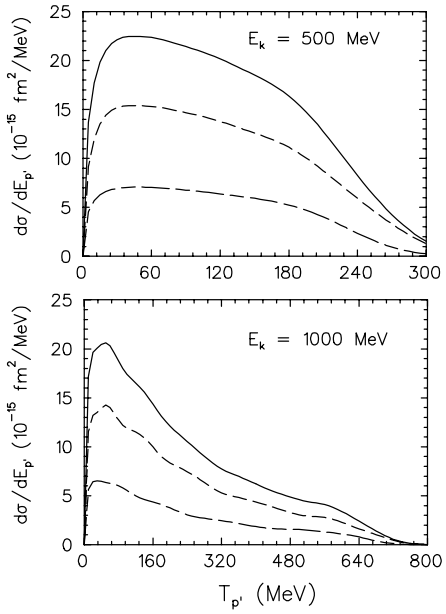

FIG. 3: Differential cross section $d\sigma/dE_{p'}$ [Eq. (27)] as a function of the outgoing proton laboratory kinetic energy $T_{p'}$. The target nucleus is ^{12}C and the incident neutrino energy is taken to be 500 and 1000 MeV. The solid line represents the cross section calculation summed over both muon helicities ($h = \pm 1$) and over both bound-state ($1s^{1/2}$ and $1p^{3/2}$) orbitals. The dashed and long-dashed–short-dashed lines represent the individual contributions to the (unpolarized muon) cross section from the $1p^{3/2}$ and $1s^{1/2}$ orbitals, respectively.

The cross section that results from adding the contributions from both muon helicities ($h = \pm 1$) and both neutron orbitals ($1s^{1/2}$ and $1p^{3/2}$) is depicted in Fig. 3 by the solid line. The dashed and long-dashed–short-dashed lines represent the calculation where we have summed over the two helicity values for the individual $1p^{3/2}$ and $1s^{1/2}$ orbitals, respectively. The result for the full cross section (solid line) may be compared to Fig. 8 of Ref. [38]. In the kinematical region in which they can be compared, there is good agreement in both the shape and magnitude of the cross sections.

Next we investigate in Fig. 4 the contribution from the single-nucleon form factors to the differential cross section for incident neutrino energies of $E_k = 500$ and 1000 MeV. As in the previous figures, the full result is displayed by the solid line. Next in importance is the long-dashed–short-dashed line obtained by setting the weak Pauli form factor to zero ($F_2 \equiv 0$). The last three lines are obtained from calculations using a single non-zero form factor. That is, the dashed line is obtained from the full calculation by setting $F_1 = F_2 = 0$, the dotted line by setting $G_A = F_2 = 0$, and the dashed-dotted line by setting $G_A = F_1 = 0$. This figure clearly illustrates the relatively minor role played by the kinematically suppressed weak Pauli form factor F_2. Indeed, by itself, it yields a partial cross section that both in magnitude and in shape shows little resemblance to the full cross section. Clearly, the two dominant form factors are the weak Dirac and the axial-vector form factors, with the latter assuming the dominant role. Yet by itself, no single form factor reproduces the full cross

section indicating that *all* interference terms, F_1F_2, F_1G_A, and F_2G_A are important for the charged-current process. Contrast this to the neutral-current process where the Dirac form factor is strongly suppressed by the weak mixing angle ($1-4\sin^2\theta_W \approx 0.076$).

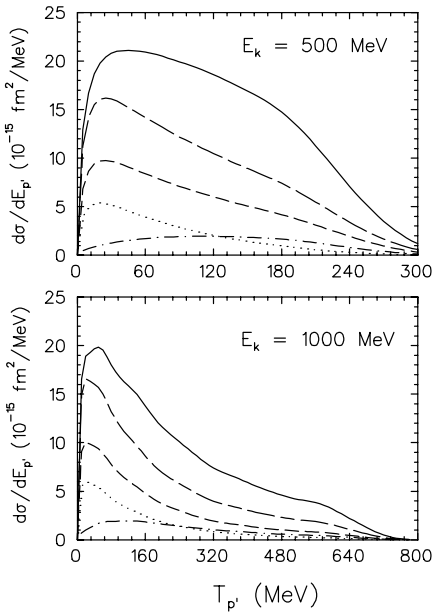

FIG. 4: Effect of the single-nucleon form factors on the differential cross section [Eq. (27)] as a function of the laboratory kinetic energy $T_{p'}$ of the outgoing proton. The calculations include a sum over the two ($1s^{1/2}$ and $1p^{3/2}$) neutron orbitals in ^{12}C and are for incident neutrino energies of 500 and 1000 MeV. Explanation for the various lines is given in the text.

As mentioned earlier, systematic errors with the neutron detection make the ratio of neutral- to charged-current reactions $R(NC/CC)$ a more viable alternative than the proton-to-neutron neutral-current ratio $R(p/n)$. Thus, we now compare in Fig. 5 the cross section for the charged-current reaction with that for the neutral-current process: $\nu+X(Z,A) \longrightarrow \nu+p+X(Z-1,A-1)$. The solid line represents the full charged-current cross section from ^{12}C, where we have summed over both bound-state orbitals and both muon helicities. The dashed line represents the corresponding neutral-current cross section with no strange-quark contribution to the spin of the proton (i.e., $g_A^s \equiv 0$); the long-dashed–short-dashed line is the same calculation with $g_A^s = -0.19$. Results are shown for incident neutrino energies of 500 MeV (top graph) and 1000 MeV (bottom graph). A comparison to Fig. 8 of Ref. [38] shows good agreement in both the shape and magnitude of the cross sections. The axial-vector form factor plays a dominant role in the neutral-current neutrino-proton reaction and makes this reaction particularly sensitive to the strange-quark contribution to the spin of the proton. Recall that the axial-vector form factor of a proton in the neutral-current case is given by [33]

$$\widetilde{G}_A(Q^2) = \Big(g_A - g_A^s\Big) G_D^A(Q^2) \underset{Q^2=0}{\longrightarrow} (1.26 - g_A^s) \underset{g_A^s=-0.19}{\longrightarrow} 1.45 \; . \tag{31}$$

Here $G_D^A(Q^2)$ is the axial-vector form factor of the nucleon (see Appendix B) and a value of $g_A^s = -0.19$ is assumed for the strange-quark contribution to the spin of the nucleon [39]; this value seems to improve the agreement with the Brookhaven National Laboratory experiment

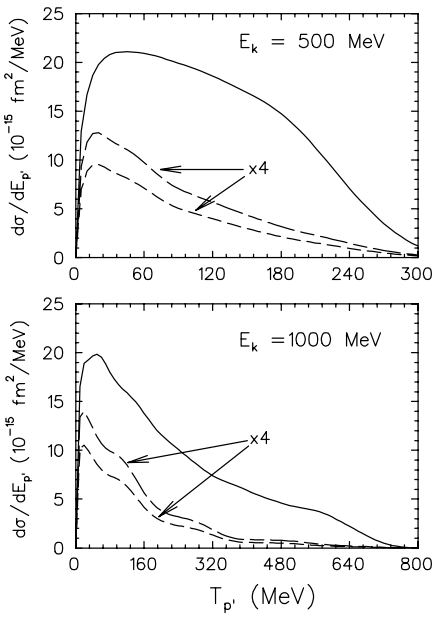

FIG. 5: Differential cross section $d\sigma/dE_{p'}$ [Eq. (27)] for neutrinos on ^{12}C as a function of the laboratory kinetic energy $T_{p'}$ of the outgoing proton. The solid line represents the full charged-current neutrino-nucleus cross section, while the dashed (long-dashed–short-dashed) line represents the corresponding neutral-current neutrino-nucleus cross section using $g_A^s=0$ ($g_A^s=-0.19$). Results are shown for incident neutrino energies of 500 and 1000 MeV. Note that for clarity the neutral-current cross sections have been multiplied by a factor of 4.

E734 [40]. Note that this negative value of g_A^s leads to an increase in the proton $\widetilde{G}_A$ by about 15%.

We are now in a position to display results for the main observable of this work: the ratio of neutral- to charged-current neutrino-nucleus scattering cross sections $R(NC/CC)$ defined in Eq. (2). For notational simplicity let us denote the differential cross section $d\sigma/dE$ by σ, where it is implied that we have summed over the $1s^{1/2}$ and $1p^{3/2}$ orbitals of ^{12}C as well as over the two values of the helicity (when appropriate). Then, because of the dominance of the axial-vector form factor we may write the NC cross sections as

$$\frac{\sigma_{NC}(g_A^s\neq 0)}{\sigma_{NC}(g_A^s=0)} \approx \left(1-\frac{g_A^s}{g_A}\right)^2 \ . \tag{32}$$

As the strange-quark contribution to the spin of the nucleon is assumed to be isoscalar, the charged-current reaction is insensitive to it. Thus,

$$\frac{R(NC/CC;g_A^s\neq 0)}{R(NC/CC;g_A^s=0)} \approx \left(1-\frac{g_A^s}{g_A}\right)^2 \underset{g_A^s=-0.19}{\longrightarrow} 1.32 \ . \tag{33}$$

That is, assuming the dominance of the axial-vector form factor in neutral-current neutrino-proton scattering, a $\sim 30\%$ enhancement (for $g_A^s=-0.19$) in $R(NC/CC)$ is expected from a non-zero strange-quark contribution to the spin of the nucleon. The $R(NC/CC)$ ratio is plotted in Fig. 6 as a function of the laboratory kinetic energy $T_{p'}$ of the outgoing proton for incident neutrino energies of 500 and 1000 MeV. The solid and long-dashed–short-dashed

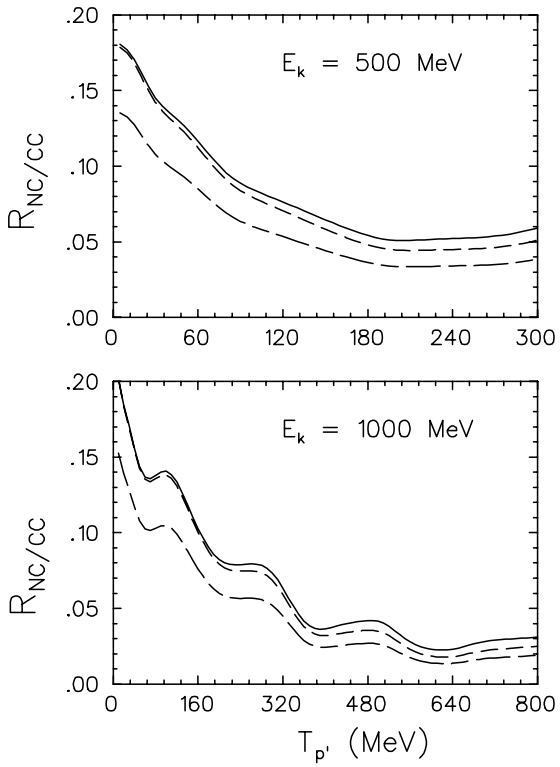

FIG. 6: Ratio of neutral- to charged-current neutrino-nucleus (^{12}C) cross sections as a function of the laboratory kinetic energy of the outgoing proton $T_{p'}$. The solid and long-dashed–short-dashed lines correspond to $g_A^s = -0.19$ and $g_A^s = 0$, respectively. The dashed line is obtained by multiplying the $g_A^s = 0$ result by a constant factor of 1.32 [see Eq. (33)]. The incident neutrino energies are 500 and 1000 MeV.

lines correspond to non-zero and zero values of g_A^s, respectively. Further, the dashed line has been obtained by multiplying the $g_A^s = 0$ result by a constant enhancement factor of 1.32. The agreement between the solid and dashed lines indicates that the simple estimate given in Eq. (33) is quantitatively correct — especially at small $T_{p'}$ (or equivalently small momentum transfer q) where the contribution from the interference term $\widetilde{F}_2\widetilde{G}_A$ remains small. While significant, the sensitivity to g_A^s in $R_{NC/CC}$ is about a factor of two less than in $R(p/n)$ where both proton and neutron NC cross sections are sensitive to g_A^s. We trust that after working out the systematic uncertainties in the neutron detection, this crucial experiment will also be performed.

We close this section with a brief comment on the mild oscillations displayed by the neutral- to charged-current ratio $R_{NC/CC}$, especially at 1000 MeV. Note that this structure is not unique to the CC cross sections (see Fig. 3) but has already been observed in the NC cross sections of Ref. [33] (see Fig. 9). As neither the momentum distribution of the bound nucleons nor the nucleon form factors display any such structure, we attribute this behavior to a kinematical effect originally pointed out in Ref. [39] (see Fig. 1) and later reproduced by us in Figs. 5-6 of Ref. [33]. The mild oscillations in the single-differential cross section $d\sigma/dT_{p'}$ is a *residual* effect associated with the existence of a "double-humped" structure in the double-differential cross section $d^2\sigma/dT_{p'}d(\cos\alpha)$ (here α is the polar angle of the outgoing proton with kinetic energy $T_{p'}$). In turn, the emergence of the double-humped

structure is a purely kinematical effect that results from the inability of the reaction to produce medium-energy nucleons. That is, high-energy neutrinos are able to produce low- or high-energy nucleons but not medium energy ones. While the double-humped structure is a robust kinematical effect, the integration over α introduces model dependences that smooth out — to a greater or lesser degree — some of the structure displayed by $d^2\sigma/dT_{p'}d(\cos\alpha)$.

IV. SUMMARY

The distribution of mass, charge, and spin in the proton are among the most fundamental properties in hadronic structure. In this context, a topic that has received tremendous attention for over fifteen years is the contribution of strange quarks to the structure of the proton. In this work we have focused on the strange-quark contribution to the spin of the proton (g_A^s). Elastic neutrino-proton scattering at low momentum transfer is particularly well suited for this study, as the axial-vector form factor of the proton — the observable that encompasses the spin structure of the proton [see Eq. (31)] — dominates this reaction. Indeed, the two "competing" Dirac and Pauli form factors are strongly suppressed, the former by the weak mixing angle ($1-4\sin^2\theta_W \approx 0.076$) and the latter by the nucleon mass ($|\mathbf{q}|/2M$). Yet in an effort to reduce systematic uncertainties related to the neutrino flux, a "ratio-method" has been proposed to extract g_A^s. Two ratios are particularly useful in this regard: a) proton-to-neutron yields in elastic neutrino scattering [Eq. (1)] and b) neutral-current-to-charged-current yields [Eq. (2)]. While the former shows a larger sensitivity to g_A^s, the latter is insensitive to systematic errors associated with neutron detection. As neutrino experiments involve extremely low count rates, these reactions use targets that consists of a combination of free protons and nucleons bound into nuclei. Thus, nuclear-structure effects must be considered.

In the present work we have extended the formalism developed in Ref. [33] for neutral-current neutrino-nucleus scattering to the charged-current reaction. In particular, cross-section ratios have been computed within a relativistic plane wave impulse approximation. Benefiting from work done by others [23, 24], we justify the omission of final-state interactions by the suggestion that while distortion effects change the overall magnitude of the cross section, they do so without a substantial redistribution of strength. Nuclear-structure effects — which enter in our formalism exclusively in terms of the momentum distribution of the bound nucleons computed at the mean-field level — were incorporated via the accurately calibrated relativistic NL3 parameter set [37]. The validity of the plane-wave approximation yields theoretical cross sections that may be displayed in closed, semi-analytic form. Although the structure of the weak hadronic current is the same for the neutral- and charged-current reactions, a few differences emerge. First, the finite muon mass results in muons produced with both negative and positive helicity. Further, a finite muon mass produces cross sections that display a sharp cut-off for low values of the incident neutrino energy. However, for the range of neutrino energies of interest to the FINeSSE collaboration (500–1000 MeV) the positive-helicity contribution becomes negligible. Further, while the same three nucleon form factors enter the neutral- and charged-current reactions, their quantitative impact differs considerably. For example, while the Dirac form factor for the neutral-current process is strongly suppressed ($\widetilde{F}_1(Q^2=0)=0.076$) it is large for the charged-current process ($F_1(Q^2=0)=1$). Hence, no single form factor dominates the charged-changing reaction. More importantly, as the strange-quark content of the nucleon is assumed to be isoscalar, the purely isovector CC reaction is insensitive to the strange-quark content of the nucleon.

This renders the ratio $R(NC/CC)$ less sensitive to strange quark effects (by about a factor of 2) than the neutral-current ratio $R(p/n)$. Still, for the value of $g_A^s = -0.19$ adopted in this work [39], a 30% enhancemenent in $R(NC/CC)$ is obtained relative to a calculation with $g_A^s = 0$. We note that our results for the charged-current cross sections were compared to similar calculations done in Ref. [38] and good agreement was found in both the shape and the magnitude of the cross section.

In summary, the sensitivity of the ratio of neutral- to charged-current cross sections to the strange-quark contribution to the spin of the nucleon g_A^s was investigated in a relativistic plane wave impulse approximation. The enormous advantage of this formalism is that our theoretical results may be displayed in closed, semi-analytic form. The central motivation behind this work is the proposed FINeSSE program that aims to measure g_A^s with unprecedented accuracy via the neutral- to charged-current ratio $R(NC/CC)$. By adopting a value of $g_A^s = -0.19$, an increase in this ratio of approximately 30% was found relative to the $g_A^s = 0$ result. While sensitive, this is less so than the corresponding ratio of proton-to-neutron yields $R(p/n)$ in neutral current neutrino-induced reactions. This measurement, however, has been hindered by difficulties associated with neutron detection. We trust that this difficulty may be overcome so that this crucial program may get off the ground.

Acknowledgments

B.I.S.v.d.V gratefully acknowledges the financial support of the University of Stellenbosch and the National Research Foundation of South Africa. This material is based upon work supported by the National Research Foundation under Grant number GUN 2048567 (B.I.S.v.d.V) and by the United States Department of Energy under Grant number DE-FG05-92ER40750 (J.P.).

APPENDIX A: LEPTONIC-HADRONIC CONTRACTION

In Sec. II A it was shown that the charged-current cross section could be expressed as the contraction of a leptonic tensor $\ell^{\mu\nu}$ [Eq. (14)] with a hadronic tensor $W^{\mu\nu}$ [Eq. (24)] written in a model-independent way in terms of thirteen independent structure functions. In this appendix we carry out the contraction, which we separate into symmetric and antisymmetric parts. That is,

$$\ell^{\mu\nu}W_{\mu\nu} = \ell^S_{\mu\nu}W^{\mu\nu}_S + \ell^A_{\mu\nu}W^{\mu\nu}_A \ . \tag{A1}$$

Here the symmetric part is given by

$$\left(\frac{4}{kE_{k'}}\right)^{-1} \ell^S_{\mu\nu}W^{\mu\nu}_S \ = \ \Big(- W_1(k\cdot K') + W_2\, f_1(q) + W_3\, f_1(P) + W_4\, f_1(p') \\ + W_5\, f_2(P,q) + W_6\, f_2(q,p') + W_7\, f_2(P,p')\Big) \ , \tag{A2}$$

while the antisymmetric part by

$$\left(\frac{4}{kE_{k'}}\right)^{-1} \ell^A_{\mu\nu}W^{\mu\nu}_A = i\Big(W_{10}\,\varepsilon^{\mu\nu\alpha\beta}k_\mu K'_\nu P_\alpha p'^\beta + W_{11}\, f_3(q,P) + W_{12}\, f_3(q,p') + W_{13}\, f_3(P,p')\Big) \ . \tag{A3}$$

Note that the following four-vector has been defined:

$$K' \equiv \frac{1}{2}(k' - h'ms) \underset{m=0}{\longrightarrow} k'\delta_{h',-1} \ . \tag{A4}$$

Further, for simplicity the following three functions have been introduced:

$$f_1(x) = 2(k\cdot x)(K'\cdot x) - x^2(k\cdot K') \ , \tag{A5a}$$
$$f_2(x,y) = (k\cdot x)(K'\cdot y) + (k\cdot y)(K'\cdot x) - (x\cdot y)(k\cdot K') \ , \tag{A5b}$$
$$f_3(x,y) = (k\cdot y)(K'\cdot x) - (k\cdot x)(K'\cdot y) \ . \tag{A5c}$$

From Eq. (A2) we see that the three structure functions W_2, W_5 and W_6 do contribute to charged-current neutrino-nucleus scattering, in contrast to the neutral-current case (see Eq. (22a) of Ref. [33]). This is due to the lack of conservation of the symmetric part of the leptonic tensor as a result of the finite muon mass [see Eq. (19a)]. Note, however, that in the massless limit $f_1(q) = f_2(P,q) = f_2(q,p') = 0$, as required. Finally, due to the form of Eq. (19b), the charged-current process remains insensitive to the two structure functions W_8 and W_9.

APPENDIX B: SINGLE NUCLEON FORM FACTORS

In Sec. II C it was shown that in the impulse approximation, the single nucleon current probed in the charge-changing reaction may be written in the following standard form:

$$\hat{J}_\mu \equiv \hat{J}^{\rm CC}_\mu - \hat{J}^{\rm CC}_{\mu 5} = F_1(Q^2)\gamma_\mu + iF_2(Q^2)\sigma_{\mu\nu}\frac{q^\nu}{2M} - G_A(Q^2)\gamma_\mu\gamma_5 \ , \tag{B1}$$

where F_1, F_2, and G_A are the Dirac, Pauli, and axial-vector form factors, respectively and the pseudoscalar form factor has been neglected. To understand the structure of the vector form

factors (F_1 and F_2) we invoke the conservation of the vector current (CVC) hypothesis. To start, one parametrizes the nucleon matrix elements of the isovector electromagnetic current in the following standard form:

$$\langle N(\mathbf{p}',s',t')|\hat{J}^{\rm EM}_\mu(T\!=\!1)|N(\mathbf{p},s,t)\rangle = \langle N(\mathbf{p}',s',t')|\overline{q}\gamma_\mu\frac{\tau_3}{2}q|N(\mathbf{p},s,t)\rangle$$
$$\overline{U}(\mathbf{p}',s')\Big[F_1^{(1)}(Q^2)\gamma_\mu + iF_2^{(1)}(Q^2)\sigma_{\mu\nu}\frac{q^\nu}{2M}\Big]U(\mathbf{p},s)\left(\tau_3\right)_{tt'}\,, \qquad \text{(B2)}$$

where $\overline{q}=(\overline{u},\overline{d})$ is an isospin doublet of quark fields, and $F_1^{(1)}$ and $F_2^{(1)}$ are the *isovector* Dirac and Pauli form factors of the nucleon, respectively. In turn, these are given in terms of proton and neutron electromagnetic form factors as follows:

$$F_i^{(1)}(Q^2) = \frac{1}{2}\left(F_i^{(p)}(Q^2) - F_i^{(n)}(Q^2)\right)\,, \quad (i=1,2)\,. \qquad \text{(B3)}$$

The CVC hypothesis is a powerful relation that assumes that the vector part of the weak charge-changing current may be directly obtained from the isovector component of the electromagnetic current. That is,

$$\hat{J}^{\rm EM}_\mu(T\!=\!1) = \hat{V}^{(3)}_\mu = \overline{q}\gamma_\mu\frac{\tau_3}{2}q\,, \quad \hat{J}^{\rm CC}_\mu(\pm) = \hat{V}^{(1)}_\mu \pm i\,\hat{V}^{(2)}_\mu = \overline{q}\gamma_\mu\left(\frac{\tau_1 \pm i\,\tau_2}{2}\right)q\,. \qquad \text{(B4)}$$

Thus, a determination of the electromagnetic form factors of the nucleon — which has been done experimentally — fixes the vector part of the charge-changing currents to:

$$\langle N(\mathbf{p}',s',t')|\hat{J}^{\rm CC}_\mu(\pm)|N(\mathbf{p},s,t)\rangle = \overline{U}(\mathbf{p}',s')\Big[F_1^{(1)}(Q^2)\gamma_\mu + iF_2^{(1)}(Q^2)\sigma_{\mu\nu}\frac{q^\nu}{2M}\Big]U(\mathbf{p},s)\left(2\tau_\pm\right)_{tt'}\,. \qquad \text{(B5)}$$

In this way the vector form factors of Eq. (B1) are then simply given by

$$F_i(Q^2) = 2F_i^{(1)}(Q^2) = F_i^{(p)}(Q^2) - F_i^{(n)}(Q^2)\,, \quad (i=1,2)\,. \qquad \text{(B6)}$$

Paraphrasing Ref. [41]: *CVC implies that the vector part of the single-nucleon matrix element of the charge-changing weak current, whatever the detailed dynamic structure of the nucleon, can be obtained from elastic electron scattering through the electromagnetic interaction!*

A similar procedure may be followed to determine the axial-vector form factor G_A in terms of the isovector axial-vector current. That is,

$$\hat{J}^{\rm CC}_{\mu 5}(\pm) = \hat{A}^{(1)}_\mu \pm i\,\hat{A}^{(2)}_\mu = \overline{q}\gamma_\mu\gamma_5\left(\frac{\tau_1 \pm i\,\tau_2}{2}\right)q\,, \qquad \text{(B7)}$$

so that

$$\langle N(\mathbf{p}',s',t')|\hat{J}^{\rm CC}_{\mu 5}(\pm)|N(\mathbf{p},s,t)\rangle \equiv G_A(Q^2)\overline{U}(\mathbf{p}',s')\gamma_\mu\gamma_5 U(\mathbf{p},s)\left(\tau_\pm\right)_{tt'}\,. \qquad \text{(B8)}$$

As before, the above expression neglects the contribution from the pseudoscalar form factor.

We finish this section by parameterizing the various nucleon form factors in terms of their known $Q^2\!=\!0$ values times form factors of a dipole form. This is identical to the procedure

employed in Appendix A of Ref. [33]) for the neutral-current reaction. We obtain

$$F_1^{(p)}(Q^2) = \left(\frac{1+\tau(1+\lambda_p)}{1+\tau}\right) G_D^V(Q^2) \ , \quad F_2^{(p)}(Q^2) = \left(\frac{\lambda_p}{1+\tau}\right) G_D^V(Q^2) \ , \tag{B9a}$$

$$F_1^{(n)}(Q^2) = \left(\frac{\lambda_n \tau(1-\eta)}{1+\tau}\right) G_D^V(Q^2) \ , \quad F_2^{(n)}(Q^2) = \left(\frac{\lambda_n(1+\tau\eta)}{1+\tau}\right) G_D^V(Q^2) \ , \tag{B9b}$$

$$G_A(Q^2) = g_A G_D^A(Q^2) \ , \tag{B9c}$$

where a dipole form factor of the following form is assumed:

$$G_D^V(Q^2) = (1 + Q^2/M_V^2)^{-2} = (1 + 4.97\tau)^{-2} \tag{B10a}$$

$$G_D^A(Q^2) = (1 + Q^2/M_A^2)^{-2} = (1 + 3.31\tau)^{-2} \tag{B10b}$$

$$\eta = (1 + 5.6\ \tau)^{-1} \quad \tau = Q^2/(4M^2) \ . \tag{B10c}$$

Finally, for reference we display the value of the various nucleon form factors at $Q^2 = 0$

$$F_1^{(p)}(0) = 1 \ , \quad F_1^{(n)}(0) = 0 \ , \tag{B11a}$$

$$F_2^{(p)}(0) = \lambda_p = +1.79 \ , \quad F_2^{(n)}(0) = \lambda_n = -1.91 \ , \tag{B11b}$$

$$G_A(0) = g_A = +1.26 \ . \tag{B11c}$$

[1] B. Kayser, Nucl. Phys.(Proc. Suppl.) **B 118**, 425 (2003).

[2] S. Eidelman et al. (Particle Data Group), Phys. Lett. B **592**, 1 (2004).

[3] C. Athanassopoulos et al. (LSND), Phys. Rev. Lett. **75**, 2650 (1995), nucl-ex/9504002.

[4] D. H. Potterveld, P. E. Reimer, B. T. Fleming, C. J. Horowitz, and R. Tayloe (FINeSE), *Physics with a near detector on the booster neutrino beam line* (2002).

[5] L. Bugel et al. (FINeSSE), *Fine-grained neutrino scattering scintillator experiment* (2003).

[6] S. Brice et al., A Proposal for a Near Detector Experiment on the Booster Neutrino Beamline: FINeSSE: Fermilab Intense Neutrino Scattering Scintillator Experiment (2004), hep-ex/0402007.

[7] A. O. Bazarko et al., Z. Phys. **C 65**, 189 (1995), hep-ex/9406007.

[8] M. Goncharov et al., Phys. Rev. **D 64**, 112006 (2001), hep-ex/0102049.

[9] D. Adams et al., Phys. Rev. **D 56**, 5330 (1997).

[10] C. B. Dover and P. M. Fishbane, Phys. Rev. Lett. **64**, 3115 (1990).

[11] R. D. McKeown, Phys. Lett. B **219**, 140 (1989).

[12] D. H. Beck, Phys. Rev. **D 39**, 3248 (1989).

[13] B. Mueller et al. (SAMPLE), Phys. Rev. Lett. **78**, 3824 (1997).

[14] K. A. Aniol et al. (HAPPEX), Phys. Rev. Lett. **82**, 1096 (1999).

[15] F. E. Maas, Eur. Phys. J. **A 17**, 339 (2003).

[16] M. J. Musolf and B. R. Holstein, Phys. Lett. **B 242**, 461 (1990).

[17] M. J. Musolf, T. W. Donnelly, J. Dubach, S. J. Pollock, S. Kowalski, and E. J. Beise, Phys. Rept. **239**, 3 (1994).

[18] C. J. Horowitz and J. Piekarewicz, Phys. Rev. **C 47**, 2924 (1993), nucl-th/9302004.

[19] S. D. Bass, R. J. Crewther, F. M. Steffens, and A. W. Thomas, Phys. Rev. **D 66**, 031901 (2002).

[20] S. D. Bass, R. J. Crewther, F. M. Steffens, and A. W. Thomas, Phys. Rev. **D 68**, 096005 (2003).

[21] G. T. Garvey, S. Krewald, E. Kolbe, and K. Langanke, Phys. Lett. **B 289**, 249 (1992).

[22] G. Garvey, E. Kolbe, K. Langanke, and S. Krewald, Phys. Rev. **C 48**, 1919 (1993).

[23] A. Meucci, C. Giusti, and F. D. Pacati (2004), nucl-th/0405004.

[24] M. Martinez, P. Lava, N. Jachowicz, J. Ryckebusch, K. Vantournhout, and J. Udias (2005), nucl-th/0505008.

[25] S. J. Barish et al., Phys. Rev. **D 16**, 3103 (1977).

[26] C. Athanassopoulos et al., Phys. Rev. **C 55**, 2078 (1997).

[27] S. Nakamura, T. Sato, V. Gudkov, and K. Kubodera, Phys. Rev. **C 63**, 034617 (2001).

[28] L. B. Auerbach et al., Phys. Rev. **C 66**, 015501 (2002).

[29] S. L. Mintz and M. Pourkaviani, Phys. Rev. **C 40**, 2458 (1989).

[30] T. S. Kosmas and E. Oset, Phys. Rev. **C 53**, 1409 (1996).

[31] C. Volpe, N. Auerbach, G. Colo, and N. Van Gial, Phys. Rev. **C 65**, 044603 (2002).

[32] C. Maieron, M. C. Martinez, J. A. Caballero, and J. M. Udias, Phys. Rev. **C 68**, 048501 (2003).

[33] B. I. S. van der Ventel and J. Piekarewicz, Phys. Rev. **C 69**, 035501 (2004), nucl-th/0310047.

[34] B. D. Serot and J. D. Walecka, Adv. Nucl. Phys. **16**, 1 (1986).

[35] F. J. Yndurain, *The Theory of Quark and Gluon Interaction* (Springer, 1999).

[36] H. Kim, J. Piekarewicz, and C. J. Horowitz, Phys. Rev. **C 51**, 2739 (1995).
[37] G. A. Lalazissis, J. Konig, and P. Ring, Phys. Rev. **C 55**, 540 (1997).
[38] W. M. Alberico et al., Nucl. Phys. **A623**, 471 (1997), hep-ph/9703415.
[39] C. J. Horowitz, H. Kim, D. P. Murdock, and S. Pollock, Phys. Rev. **C48**, 3078 (1993).
[40] L. A. Ahrens et al., Phys. Rev. **D 35**, 785 (1987).
[41] J. D. Walecka, *Theoretical Nuclear and Subnuclear Physics* (Oxford University Press, 1995).